Available online at www.sciencedirect.com
SCIENCE DIRECT®
International Journal of Pharmaceutics 250 (2003) 169–180
international journal of pharmaceutics
www.elsevier.com/locate/ijpharm

Absorption into silicone rubber membranes from powders and aqueous solutions

Kelly D. McCarley, Annette L. Bunge *

Chemical Engineering Department, Colorado School of Mines, Golden, CO 80401, USA

Received 26 August 2001; received in revised form 26 August 2002; accepted 17 September 2002

Abstract

This study compared the rate and amount of absorption from aqueous solutions and pure powders of 3- and 4-cyanophenol (CP) into silicone rubber (SR) membranes. SR membranes were cast directly onto a zinc-selenide attenuated total reflectance (ATR) crystal, which was then mounted on a Fourier transform infrared (FTIR) spectrometer. CP was presented to the SR membrane from aqueous solutions or powders sufficient to completely cover the membrane surface. The concentration of CP in the membrane at the interface with the crystal was determined by IR absorption of the C≡N stretch. The amount of CP in the SR membrane at steady state was determined by extraction and UV absorption measurements of the extract. The concentration of CP in SR membranes was found to depend weakly on the concentration of the aqueous solution. The amount of CP in SR membranes equilibrated with pure powders was essentially the same as for the CP-saturated solutions. Diffusion coefficients for 3 and 4-CP (2.8 ± 0.2 and $2.5 \pm 0.6 \times 10^{-7}$ cm^2 s^{-1}, respectively) were not statistically different. The absorption rate of CP into SR membranes was almost the same from the powder and aqueous solution indicating that the rate of mass transfer from the powder to membrane was larger than 0.04 cm h^{-1}.

Keywords: Silicone rubber; ATR-FTIR; Membrane; Cyanophenol; Absorption; Diffusion coefficients

1. Introduction

Dermal absorption of small organic compounds is a solution-diffusion process. Thus, dermal absorption rates depend on the partition coefficient between the topically applied chemical and skin as well as the diffusion coefficient of the chemical in skin. If the topical formulation is a liquid, then the formulation is in intimate contact with the skin surface and for typical dermal absorption rates local equilibrium should be established at this interface. However, when a chemical is applied to skin as a powdered solid, then it is possible that local equilibrium can only occur where the solid particles directly contact the skin.

The goal of this investigation was to examine experimentally the mechanisms controlling the

* Corresponding author. Tel.: +1-303-273-3722; fax: +1-303-273-3730
E-mail address: abunge@mines.edu (A.L. Bunge).

0378-5173/02/$ - see front matter
PII: S0378-5173(02)00538-0

rate and extent of absorption from powdered solids, particularly compared with liquid exposures. Specifically absorption was measured following exposure of aqueous solutions and pure powder of test chemicals (the meta and para isomers of cyanophenol (CP)) to silicone rubber (SR) membranes, which simulated skin. Absorption rates were measured using attenuated total reflectance-Fourier transform infrared (ATR-FTIR) spectrometer following procedures defined in several previous publications (Farinas et al., 1994; Fieldson and Barbari, 1993, 1995; Pellett et al., 1997a,b; Watkinson et al., 1994).

The ATR-FTIR experiment is shown schematically in Fig. 1. A membrane is placed in intimate contact with the ATR crystal, and the chemical solution or powder is placed on top of the membrane at the beginning of the experiment. Chemical diffuses through the membrane until it reaches the surface of the ATR crystal. An IR beam passes through the crystal (which has beveled edges at a specified angle) and is reflected several times. An evanescent wave penetrates into the membrane producing a spectrum. The depth of penetration is on the order of 1 μm, but depends on the refractive indices of the crystal and membrane, the beveled angle and the wavelength of the IR beam. Absorbance of the chemical is monitored by tracking the absorbance peak that is characteristic of the chemical.

2. Theory

Fickian diffusion of a chemical through a homogeneous, non-porous membrane of thickness L, with a constant partition coefficient is described by the differential mass balance:

$$\frac{\partial C_{\mathrm{m}}}{\partial t} = D\frac{\partial^2 C_{\mathrm{m}}}{\partial x^2} \quad \text{for } 0 < x < L \tag{1}$$

where C_{m} is the concentration of diffusing chemical in the membrane m, D is the chemical diffusion coefficient through the membrane, x is the position in the membrane, and t is the time since the chemical exposure to the membrane began. In the ATR-FTIR experiments, the SR membrane is initially chemical free (i.e. $C_{\mathrm{m}} = 0$ for $0 < x < L$ at $t = 0$) and no chemical absorbs into the ATR crystal at the membrane–crystal (i.e. $\partial C_m/\partial x = 0$ at $x = L$ for all t).

Solid chemicals or chemicals deposited on solid carriers (vehicles) may make poorer contact with the membrane than do liquid chemicals or chemicals dissolved in liquid vehicles. This may introduce an additional mass transfer resistance which is mathematically represented by requiring the flux at the vehicle–membrane interface to be proportional to a mass transfer coefficient k_{v}. That is,

$$-D\frac{\partial C_{\mathrm{m}}}{\partial x} = k_{\mathrm{v}}(K_{\mathrm{m/v}}C_{\mathrm{v}}^0 - C_{\mathrm{m}}) \quad \text{at } x = 0 \tag{2}$$

where $K_{\mathrm{m/v}}$ is the equilibrium partition coefficient between the membrane and vehicle, and C_{v}^0 is the concentration of the chemical in the vehicle (which is constant in all the experiments described here). If the mass transfer resistance ($1/k_{\mathrm{v}}$) is very large, then no chemical will transfer into skin (i.e. $\partial C_{\mathrm{m}}/\partial x = 0$). If the resistance is very small, then local equilibrium will exist (i.e. $C_{\mathrm{m}} = K_{\mathrm{m/v}}C_{\mathrm{v}}^0$). Note that penetration rates from saturated aqueous solutions and from pure powders would be the same if local equilibrium were established at the chemical/membrane interface.

The following equation describing the chemical concentration at the interface of the membrane–ATR crystal (i.e. at $x = L$) was derived by solving Eq. (1) for the listed restricting conditions (Fieldson and Barbari, 1995):

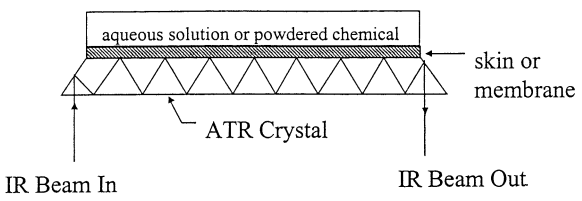

Fig. 1. Schematic diagram of the ATR-FTIR experiment.

$$\frac{C_m}{(K_{m/v}C_v^o)} = \left[1 - 2\alpha_v \sum_{n=1}^{\infty} \times \frac{\alpha_v \sin \lambda_n + \lambda_n \cos \lambda_n}{\lambda_n(\alpha_v^2 + \alpha_v + \lambda_n^2)} \exp\left(-\frac{\lambda_n^2 Dt}{L^2}\right)\right] \quad \text{at } x = L \tag{3}$$

In this equation, $\alpha_v = k_v L/D$ and the eigenvalues are the infinite number of positive roots satisfying the expression $\lambda_n + \alpha_v \tan = 0$. If the vehicle does not present a mass transfer resistance (i.e. $1/k_v = 0$ and $\alpha_v \to \infty$), Eq. (3) simplifies to give (Crank, 1979; Fieldson and Barbari, 1993, 1995):

$$\frac{C_m}{(K_{m/v}C_v^0)} = \left[1 - 2\sum_{n=1}^{\infty} \frac{\sin \lambda_n}{\lambda_n} \exp\left(-\lambda_n^2 \frac{Dt}{L^2}\right)\right] \tag{4}$$

where $\lambda_n = (2n+1)\pi/2$. After a long time, both Eqs. (3) and (4) predict that $C_m = K_{m/v}C_v^0$ at $x = L$. Also, both Eqs. (3) and (4) were developed assuming the partition coefficient between the membrane and vehicle is constant.

Fig. 2 shows the effect of increasing the mass transfer resistance on the concentration in the membrane at the membrane–crystal interface as predicted by Eq. (3). As the mass transfer resistance increases, the time to reach steady state is increased due to the additional lag time in the vehicle. Note that the vehicle mass transfer resistance will have a minimal effect if α_v is larger than about 1.

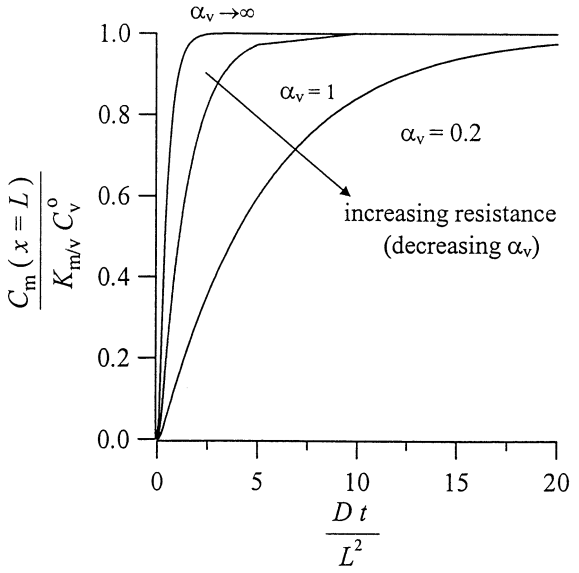

Fig. 2. Effect of increasing vehicle mass transfer resistance on concentration at the membrane–crystal interface.

Fieldson and Barbari (1993, 1995) relate the concentration in the membrane to the ATR-FTIR absorbance measurements using the Beer–Lambert law. Based on calculations described by Farinas et al. (1994), the penetration depth of the IR beam into the SR membrane is expected to be ~1 μm, which is significantly less than the total thickness of the SR membrane (approximately 200 μm). Thus, the IR spectra should represent conditions in the SR membrane at the interface between the membrane and the ATR crystal. Consequently,

$$\frac{A}{A_f} = \frac{C_m}{K_{m/v}C_v^0} \quad \text{at } x = L \tag{5}$$

where A is the IR absorbance measured as peak area and A_f is A after steady state (or in this case, equilibrium) is reached.

3. Materials and methods

The relevant physical properties of 3-cyanophenol (3CP) and 4-cyanophenol (4CP) are listed in Table 1. These chemicals were chosen because the stretch of the cyano functional group (C≡N) absorbs in the IR region between wave numbers 2260–2190 cm^{-1}, where skin and SR are transparent. Both 3CP and 4CP were reagent grade and purchased from Aldrich Chemical (Milwaukee, WI). Sylgard 184 2-part SR elastomer (Dow Corning, Auburn, MI) was purchased from Krayden, Inc. (Denver, CO). All aqueous solutions were prepared using high purity water (deionized water treated further by a Millipore Milli-Q Reagent water system, Bedford, MA).

3.1. Membrane preparation

SR membranes were cast directly on the ATR crystal to ensure adequate contact between the

Table 1
Physical properties of chemicals in this study

Chemical name	Abbreviation	MW	$\log_{10} K_{o/w}$	Solubility in water (mg ml^{-1})[a]	T_{mp} (°C)
3-Cyanophenol	3CP	119.2	1.61	29	79–81
4-Cyanophenol	4CP	119.2	1.60	12.5	110–113

[a] As determined by UV absorption.

membrane and the crystal. The SR mixture was prepared by mixing one part of the Sylgard silicone-curing agent with ten parts of the Sylgard silicone elastomer, then degassed at room temperature and 27 in Hg vacuum for 30 min. A cardboard template ($\sim$1 mm thick) with an opening of 3×10 cm was glued onto the ATR crystal holder. The opening in the template was larger than and centered on the ATR crystal.

After degassing, the SR mixture was poured onto the ATR crystal, filling the template. A glass-mounting slide was used to scrape and level the SR mixture within the template and any excess SR mixture was removed. After curing the SR mixture on the ATR crystal (5 h at 20 in Hg vacuum and 170 °F), the cardboard template was removed.

Following the absorption and partition coefficient measurements, the membrane was peeled from the crystal and the thickness of each membrane determined using a digital vernier caliper (Mitutoyo Series 500-115). Measurements were taken at 5 points along the membrane and the results were averaged. The standard deviation for a single membrane was always less than 20 μm. The membranes were between 188 and 285 μm thick, with an average of 228 μm ($\pm$28 μm) for the 17 membranes used in the absorption experiments.

3.2. Absorption experiments

The ATR-FTIR experimental system, illustrated in Fig. 1, was similar to that described by Farinas et al. (1994), Pellett et al. (1997a,b), Watkinson et al. (1994). The horizontal ATR accessory (Contact Sampler^{TM}, Spectra-Tech Inc., Shelton, CT) supports a zinc-selenide (ZSe) internal reflection crystal ($7.5 \times 1 \times 0.2$ cm) with a 45° incident angle on a Biorad (Cambridge, MA) FTS 40 FTIR.

Chemicals were presented to the SR membrane from either (1) aqueous solutions or (2) powder of the pure chemical. The powder was crushed with a mortar and pestle and then sieved. Only the 38–65 μm fraction was used in these experiments.

For each absorption run, a background spectra was collected after which chemical was placed onto the membrane. Aqueous solutions were poured directly onto the membrane and then covered to prevent evaporation. Powdered chemicals, sufficient to completely cover the membrane with at least a layer of densely packed particles were spread onto the membrane, and either left uncovered (unoccluded) or covered (occluded) with a glass slide and aluminum foil, held in place with duct tape. IR spectra were taken every 30 s for the first 10 min (20 data sets), every minute for the next 20 min (20 data sets), then every 5 min for the next 1.5 h (20 data sets) or 3 h (40 data sets) for the powdered CP runs. Each data set consisted of 10 scans.

The absorption of 4CP from a 10 mg g^{-1} aqueous solutions was measured on each membrane as a calibration of that membrane. Following each run (except for the last), the chemical was removed, and the membrane was cleaned with high purity water, which was left on the membrane for at least 30 min. The water was removed, and the membrane was air-dried. Before starting the next run, an IR spectrum was taken to ensure that all CP and water was removed from the membrane. After the last run, the equilibrated membrane was used to measure the partition coefficient.

3.3. Partition coefficient measurements

The partitioning of chemical into the membrane was determined by measuring the concentration of

CP in a SR membrane after it had equilibrated with a known concentration of an aqueous CP solution (C_v). Following the last absorption run for each membrane, the SR membrane was patted dry, peeled from ATR crystal, and placed into a known mass of 0.01 M sodium hydroxide solution to extract the chemical. The pH of the NaOH solution was large enough to fully ionize all extracted CP with no perceptible change in the solution pH. After at least 24 h, the membrane was removed from the NaOH solution, dried and then weighed. The concentration of chemical in the NaOH solution was measured with the UV spectrophotometer (Hewlett–Packard 8451 Diode Array) at 276 nm for 4CP and 222 nm for 3CP. The UV was calibrated using known amounts of 3 and 4CP prepared in 0.01 M NaOH solutions. A second extraction demonstrated that CP was completely removed from the membrane in the first extraction.

A similar procedure was used to determine the amount of 4CP in the SR membrane equilibrated with either saturated water or powder. However, prior to exposure of the SR membrane to the chemical, an additional SR membrane was placed into direct contact with the first SR membrane to prevent solid chemical from sticking to the first membrane. This was done because the presence of any solid chemical on the first membrane would dramatically change C_m estimated by the extraction technique. The presence of the additional SR membrane increased the time required to reach equilibrium but not the equilibrium amount of CP in the first SR membrane at equilibrium. Once equilibrium was achieved and the chemical is removed, the second membrane was removed and the first membrane analyzed for CP. The solubility limits of 3CP and 4CP in water (listed in Table 1) were determined by UV spectrophotometer.

4. Results and discussion

As shown in Fig. 3, absorption peak heights at the designated UV wavelengths were linearly related to CP concentration for solutions of 4CP less than 6 mg g^{-1} and for 3CP solutions less than 10 mg g^{-1}. The error bars for replicated measurements are smaller than the data symbols.

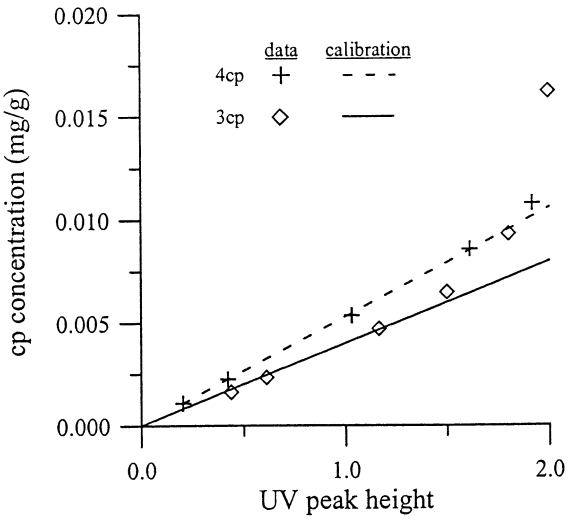

Fig. 3. UV calibration curves for 3CP (222 nm) and 4CP (276 nm) in 0.01 NaOH solution.

Fig. 4 shows C_m, determined by extraction and UV, as a function of C_v. In addition, for saturated 4CP vehicles $C_m = 0.75 \pm 0.04$ mg g^{-1} ($n = 3$), and for powdered 4CP vehicles $C_m = 0.715 \pm 0.0006$ mg 4CP g^{-1} membrane ($n = 2$). As demonstrated in Fig. 4, C_m is represented better by the nonlinear

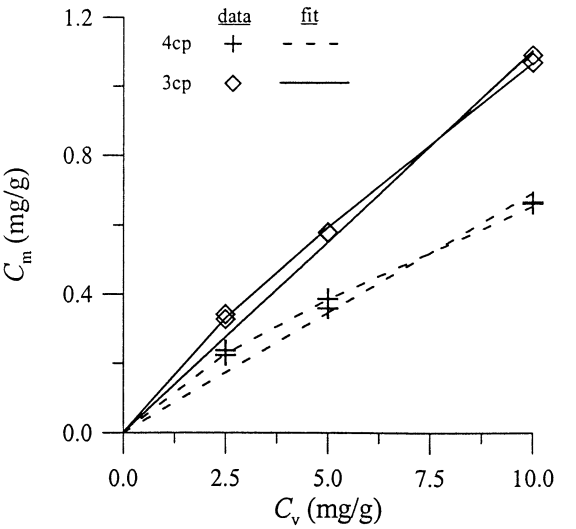

Fig. 4. C_m as a function of C_v for aqueous solutions of 3 and 4CP.

Freundlich isotherm equation:

$$C_m = aC_v^{\gamma} \quad (6)$$

(where $a = 0.11$ and $\gamma = 0.76$ for 4CP and $a = 0.15$ and $\gamma = 0.85$ for 3CP) than by a linear regression forced through the intercept:

$$C_m = bC_v \quad (7)$$

(where $b = 0.069$ for 4CP and 0.111 for 3CP). Note that a and b were calculated using consistent units for C_m and C_v (mg g^{-1}). These data indicate that the partition coefficient varies slightly with C_v. Thus, $K_{m/v}$ for 4CP at 10 mg g^{-1} is approximately 70% of the value for 2.5 mg g^{-1} solutions (0.063 compared with 0.081). For 3CP, $K_{m/v}$ at 10 mg g^{-1} is about 80% of the value for 2.5 mg g^{-1} (0.11 compared with 0.13). Pellett et al. (1997a) reported a constant partition coefficient for 4CP between SR and water of 0.132. This is similar to the partition coefficient values measured here. The difference is probably due to differences in the SR materials.

The melting point of 3CP is lower than for 4CP (Table 1), which causes the solubility of 3CP in water to be larger than for 4CP (Prausnitz et al., 1986). If partitioning into the SR were similar for 3 and 4CP, then the amount of 3CP in the membrane for a given vehicle concentration would be the same as for 4CP in equilibrium with the same vehicle concentration. However, as demonstrated in Fig. 4, the SR–water partition coefficient for 3CP was larger than for 4CP, suggesting that the solubility of 3CP in SR is larger than expected based on the differences of aqueous solubilities for 3 and 4CP.

Fig. 5 shows ATR-FTIR spectra from two separate absorption experiments on the same membrane. In one experiment, a saturated aqueous solution of 4CP was applied to the SR surface, while in the other experiment only water was used. The spectra shown in Fig. 5, including the expanded view of the CP peak in Fig. 5b, were collected 30 min after the start of each experiment. Prior to the start of these experiments, the FTIR absorbance for water (i.e. peak height between 4000 and 2700 cm^{-1}) and for CP (i.e. 2600–2190 cm^{-1}) were at baseline values. These results illustrate that water absorbs into the SR membrane along with CP, and that the presence of 4CP did not alter the rate of water absorption (as indicated by FTIR absorbance). Fig. 5 also demonstrates that the water peak does not interfere with the CP peak.

Fig. 6 shows a typical set of absorption experiments conducted on the same membrane for three values of C_v: 2.5, 5 and 10 mg of 4CP g^{-1} water. Each data point is the average absorbance of the 4CP peak (A) from ten scans. The absorption reached equilibrium after approximately 50 min as indicated by either a plateau or a significant decrease in the rate of increase in A. As discussed later, the slow upward drift in the peak area after equilibrium was apparently reached seemed to correlate with growth of the water peak. For consistency, the final absorbance (A_f) was defined as the average of the last 3 data points in each run.

The FTIR peak areas (A) were generally reproducible in replicated experiments on the same membrane. However, replicated experiments on different membranes did not always generate reproducible values for A. This is evident from the results in Fig. 7, which report the final peak area, A_f, as a function of C_v for all experiments performed with aqueous solutions of 3 and 4CP. Even though C_v and C_m were directly related (see Fig. 4), A_f varied by almost a factor of 2 for 4CP when C_v was 10 mg g^{-1}. However, when A_f from all experiments for a given membrane were normalized by A_f from the calibration run (i.e. $C_v =$ 10 mg 4CP g^{-1}) for that membrane, $A_{f,10}$, then $A_f/A_{f,10}$ was approximately proportional to C_v^{γ} as shown in Fig. 8.

Pellett et al. (1997a) reported that A_f for saturated 4CP solutions diffusing through SR membranes was reproducible between membranes that were pre-saturated (with $n = 3$) ot that were untreated ($n = 3$) for pre-saturated membranes. when the SR membranes were pre-saturated with water for 48 h, A_f was 1.75 times smaller than for membranes that were not pre-saturated with water. Pellett et al. speculated that pre-saturating the membranes with water may have caused the plasticizers and fillers to be leached out of the SR, thereby, reducing the membrane's capacity to hold 4CP. In our experiments, we did not notice a difference in A_f between membranes that had been

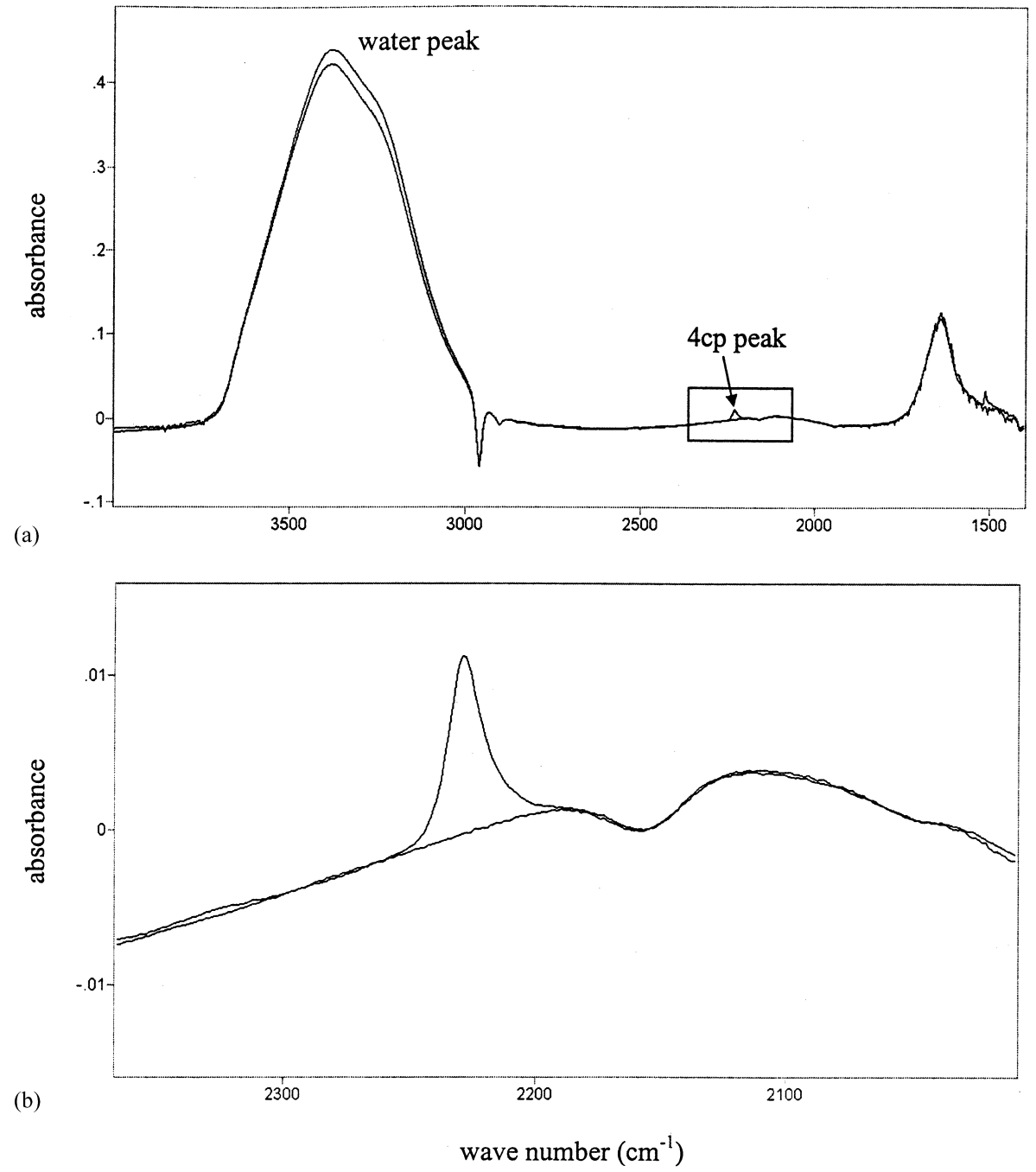

Fig. 5. ATR-FTIR spectra 30 min after application of either water or saturated aqueous solution of 4CP to the same membrane: (a) full range of wavelengths considered and (b) expanded view of the 4CP peak area (2260–2190 cm^{-1}).

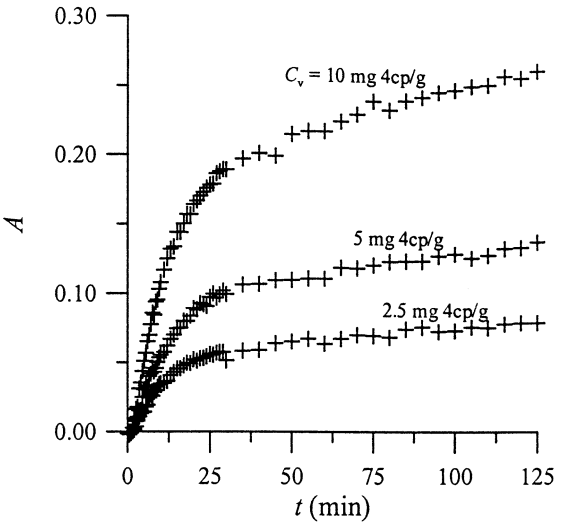

Fig. 6. Absorbance (A) plotted as a function of time for three concentrations of 4CP in water.

pre-saturated with water and membranes that were untreated. However, we used a different source of SR, which probably did not contain fillers and plasticizers.

The results from all of the absorption experiments with aqueous solutions are shown in Fig. 9a for 3CP and Fig. 9b for 4CP. Fig. 9 presents A/A_f as a function of t/L^2 where t is time in hrs and L is the measured thickness of the membrane in mm. Time was normalized by L^2 to account for variations in membrane thickness. Neglecting the weak nonlinear variation in the partition coefficient, the diffusion coefficients for 3CP and 4CP were determined to be 2.8 ($\pm$0.2) $\times 10^{-7}$ and 2.5 ($\pm$0.6) $\times 10^{-7}$ cm^2 s^{-1}, respectively, by separately fitting each set of absorption data in Fig. 9 to Eq. (4) using the statistical program JMP (SAS Institute, North Carolina), and then averaging the individual values. The quantities in parentheses designate $\pm$ one standard deviation of the diffusion coefficients. The results of the JMP analysis are detailed elsewhere (McCarley, 1999). These diffusion coefficients are within the same order of magnitude as the value of 2×10^{-7} cm^2 s^{-1} reported by Pellett et al. (Pellett et al., 1997a) for 4CP in SR. As expected for isomers, diffusion coefficients for 3CP and 4CP in SR were not

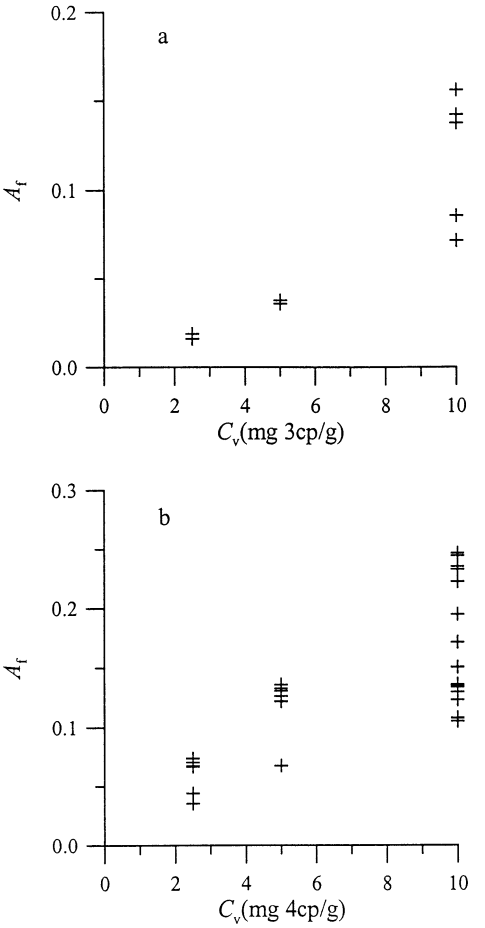

Fig. 7. A_f as a function of C_v for aqueous solutions of (a) 3CP and (b) 4CP.

significantly different. The curves in Fig. 9 represent the theoretical predictions based on the best-fit regression of D.

Fig. 10 shows the rate of absorption of 3 and 4CP into SR membranes from pure powdered (38–65 μm) chemical. All data are from experiments with occulusion, except for those identified by circles, which were unoccluded. While no major difference in the rate or extent of absorption is apparent, the unoccluded experiments appear to exhibit more scatter. The curves shown in Fig. 10 represent the same theoretical predictions as in Fig. 9. These show that the rate of CP absorption is approximately the same as for the aqueous solutions, indicating there are no mass transfer limitations associated with the solid vehicle.

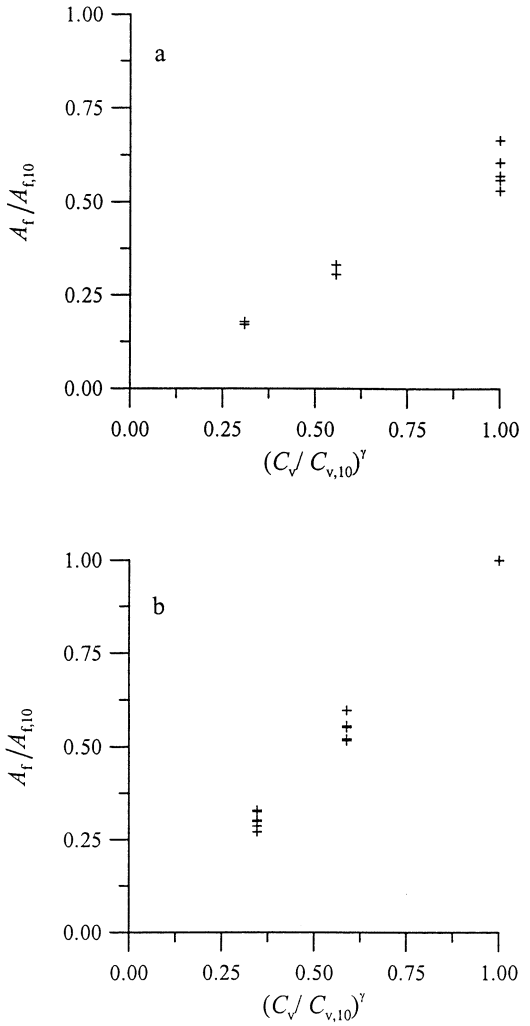

Fig. 8. $A_f/A_{f,10}$ as a function of $(C_v/C_{v,10})^\gamma$ for (a) 3CP and (b) 4CP.

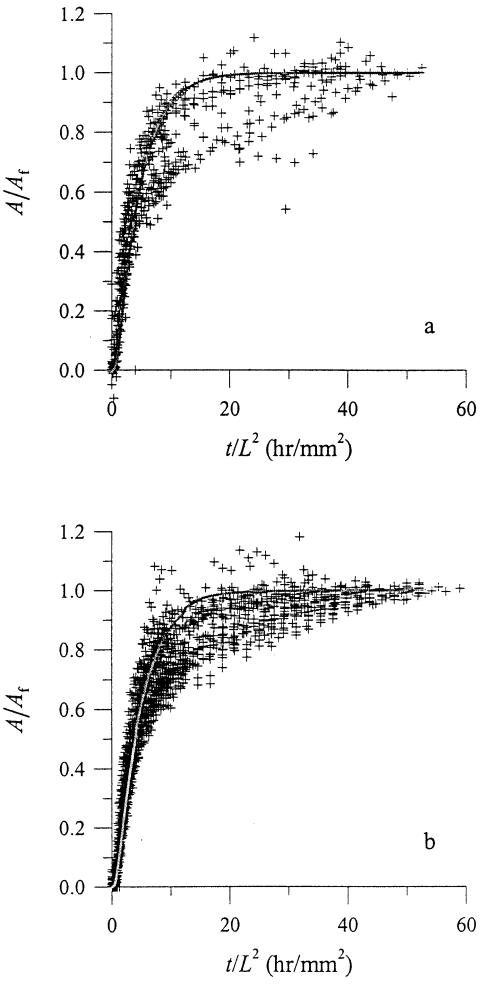

Fig. 9. A/A_f as a function of t/L^2 (h mm^{-2}) for aqueous solutions of (a) 3CP and (b) 4CP.

Since mass transfer resistances from the powders were not apparent, we can expect that α_v must be larger than 1 for these membranes. Thus, k_v for these powders is greater than D/L, which was approximately 0.04 cm h^{-1} for 4 and 3CP. In separate in vivo experiments, Pirot et al. (1997) and Reddy et al. (2002) measured lag times (i.e. $L^2/(6D)$) of about 0.6 h for 4CP in human stratum corneum. Assuming L is about 15 μm (Reddy et al., 2002), then D/L for human stratum corneum is approximately 0.0004 cm h^{-1}, meaning that α_v for human skin would be about 100 times larger than for the SR membranes studied here. Consequently, we would expect that the mass transfer resistances from 3 and 4CP powders should be even less important for human skin than in the SR membranes studied here.

This is consistent with previous in vitro diffusion cell measurements on hairless mouse skin, for which lag times from saturated aqueous solutions of 4CP and from powdered 4CP were similar (Touraille et al., 2002). In these same experiments, Touraille et al. observed that the steady-state flux from powdered solid was about 1/7th of that from a saturated aqueous solution.

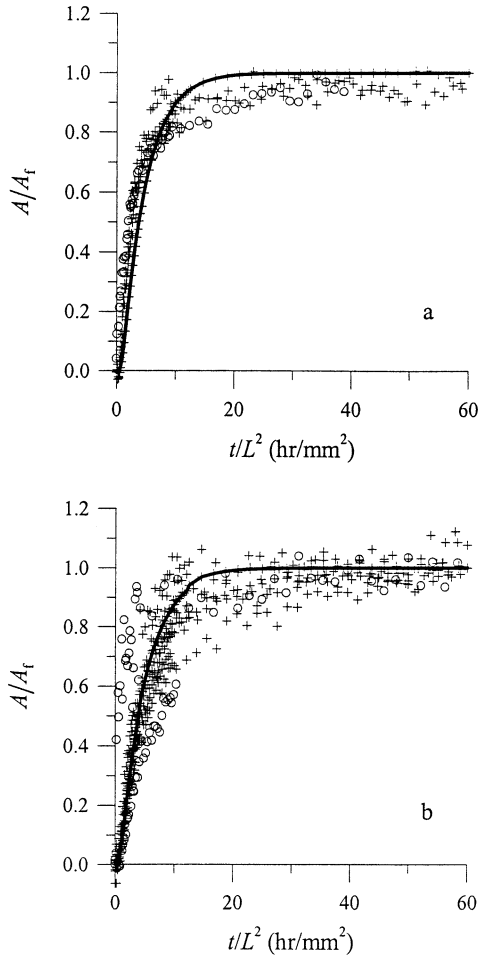

Fig. 10. A/A_f as a function of t/L^2 (h mm^{-2}) for (a) powdered 3CP and (b) powdered 4CP (+) with occlusion and (○) without occlusion.

The ratios of A_f for the occluded powdered chemical absorption runs to $A_{f,10}$ are listed in Table 2. The ratio $A_f/A_{f,10}$ is then multiplied by the ratio $C_{m,10}/C_{m,sat}$, calculated from Eq. (6), to estimate how A_f from the solid would compare with A_f from a saturated aqueous vehicle. As there is no-flux at the membrane–crystal interface, the amount of chemical in the membrane at equilibrium is expected to be the same from a powdered solid and a saturated aqueous solution, even if vehicle resistance was a factor. However, as seen in Table 2, A_f from the powders were always less than what would be expected from the saturated aqueous solutions, by a factor of ~ 0.4 for 4CP and ~ 0.2 for 3CP on average. One explanation is that water absorbed into or through the membrane affects A_f for the experiments with aqueous solutions.

We know from the UV measurements that C_m is constant for a given C_v, even if A_f is not. Also, C_m resulting from exposure to a saturated aqueous solution is approximately the same as C_m from the powdered chemical. Consequently, the presence of water in the membrane does not change the amount of chemical in the membrane. However, the IR sensitivity to CP appears to change in the presence of water, perhaps by changing the refractive index of the SR membrane. Alternatively, if membrane adherence with the ATR crystal was not always perfect, then small amounts of water might transfer across the membrane and accumulate between the crystal and membrane at one or more of the sampling points for the IR beam, which would then affect the IR signal. Typically, the height of the IR water peak (i.e. between 3000 and 3300 cm^{-1}) increased during the experiment from a starting value of essentially zero. Notably, while the time variation of the water peak was similar in repeated experiments on a single membrane, it varied between the various membranes suggesting that different membranes either absorbed or transported different amounts of water. If so, this may explain some of the data scatter observed in Fig. 9, particularly at larger values of t/L^2 where more variation in the amount of absorbed water may have occurred. We always observed more drift in the absorption experiments that had larger IR water peaks. Further investigation is required to fully understand these results.

5. Conclusions

The equilibrium concentration of 3 and 4CP in SR membranes is a weak function of the vehicle concentration represented as $C_m = aC_v^\gamma$ where a = 0.11 and $\gamma = 0.76$ for 4CP and $a = 0.15$ and $\gamma = 0.85$ for 3CP, indicating that the SR–water partition coefficients are weak functions of C_v. The partition coefficient for 3CP was larger than for 4CP, suggesting that the solubility of 3CP in SR is

Table 2
$A_f/A_{f,10}$ for powdered 4CP and 3CP

Membrane number	4CP		3CP	
	$A_f/A_{f,10}$	$(A_f/A_{f,10})(C_{m,10}/C_{m,sat})$	$A_f/A_{f,10}$	$(A_f/A_{f,10})(C_{m,10}/C_{m,sat})$
1	0.300	0.253	–	–
	0.552	0.466		
2	0.359	0.303	–	–
	0.438	0.369		
	0.399	0.336		
10	0.695	0.586	0.558	0.226
			0.611	0.248
16	0.441	0.372	0.575	0.234
			0.406	0.165
Average	0.455	0.383	0.538	0.218

$C_{m,i}$ is calculated from Eq. (6) with the regression values for 3 and 4CP, where i is the vehicle concentration (either 10 mg g^{-1} or saturated values from Table 1). $C_{m,10}/C_{m,sat}$ is equal to 0.406 for 3CP and is equal to 0.843 for 4CP.

larger than expected based on the differences of aqueous solubilities for 3 and 4CP.

Experimental results from absorption of 3 and 4CP in aqueous vehicles through SR membranes are consistent with theoretical predictions of absorption into a membrane when there is no mass transfer resistance in the vehicle. The diffusion coefficient for both 3CP and 4CP in SR was estimated at 3.0×10^{-7} cm^2 s^{-1}. The absorption rate of CP into the SR membranes studied here was about the same from solids as for aqueous solutions suggesting that there was no mass transfer resistance associated with the powdered solids. Since D/L for 4CP through these SR membranes was about 100 times larger than for human skin, one would expect that any mass transfer resistance associated with powdered 4 or 3CP would be even less significant for human skin.

The final IR absorbance A_f from the 10 mg CP g^{-1} aqueous solutions was always larger than the A_f from the powdered chemicals. However, the amount of CP in membranes equilibrated with saturated aqueous solutions and pure powders are essentially the same. This suggests that water absorption into the membrane may increase the IR sensitivity to CP, perhaps by changing the refractive index of the SR membrane. Investigations to understand these observations more fully are continuing.

6. Nomenclature

A	peak area
A_f	final peak area
$A_{f,10}$	final peak area for the 10 mg 4CP g^{-1} aqueous solution
ATR	attenuated total reflectance
CP	cyanophenol
C_m	concentration of chemical in SR membrane
C_v^0	concentration of chemical in the vehicle (constant)
D	diffusion coefficient of chemical in membrane
FTIR	Fourier transform infrared spectroscopy
$K_{m/v}$	partition coefficient of a chemical between vehicle and membrane
k_v	mass transfer coefficient for the vehicle
L	membrane thickness
SR	silicone rubber
t	time
x	position in membrane
UV	ultraviolet
ZSe	zinc selinide
α_v	dimensionless ratio of the mass transfer coefficient k_v and D/L, Eq. (3)

Acknowledgements

This work was supported in part by the US Environmental Protection Agency (Assistance Agreement Nos. CR822757, CR824053 and R826684), the US Air Force Office of Scientific Research (F49620-95-1-0001 and F49620-98-1-0060) and the National Institute of Environmental Health Sciences (ES06825). We thank M.B. Reddy, D. Macalady and K.C. McCarley for their valuable suggestions.

References

Crank, J., 1979. The Mathematics of Diffusion, second ed.. Clarendon Press, Oxford, UK.

Farinas, K.C., Doh, L., Venkatraman, S., Potts, R.O., 1994. Characterization of solute diffusion in a polymer using ATR-FTIR spectroscopy and bulk transport techniques. Macromolecule 27, 5220–5222.

Fieldson, G.T., Barbari, T.A., 1993. The use of FTIR-ATR spectroscopy to characterize penetrant diffusion in polymers. Polymer 34, 1146–1153.

Fieldson, G.T., Barbari, T.A., 1995. Analysis of diffusion in polymers using evanescent field spectroscopy. Am. Inst. Chem. Eng. J. 41, 795–804.

McCarley, K.D., 1999. Modeling chemical absorption into skin: theoretical and experimental considerations. Ph.D., Colorado School of Mines, Golden, CO.

Pellett, M.A., Watkinson, A.C., Hadgraft, J., Brain, K.R., 1997. Comparison of permeability data from traditional diffusion cells and ATR-FTIR spectroscopy. Part I. Synthetic membranes. Int. J. Pharm. 154, 205–215.

Pellett, M.A., Watkinson, A.C., Hadgraft, J., Brain, K.R., 1997. Comparison of permeability data from traditional diffusion cells and ATR-FTIR spectroscopy. Part II. Determination of diffusional pathlengths in synthetic membranes and human stratum corneum. Int. J. Pharm. 154, 217–227.

Pirot, F., Kalia, Y.N., Stinchcomb, A.L., Keating, G., Bunge, A.L., Guy, R.H., 1997. Characterization of the permeability barrier of human skin in vivo. Proc. Natl. Acad. Sci. USA 94, 1562–1567.

Prausnitz, J.M., Lichtenthaler, R.N., Azevedo, E.G., 1986. Molecular Thermodynamics of Fluid-Phase Equilibria, second ed.. Prentice Hall, Englewood Cliffs.

Reddy, M.B., Stinchcomb, A.L., Guy, R.H., Bunge, A.L., 2002. Determining dermal absorption parameters in vivo from tape stripping data. Pharm. Res. 19, 292–297.

Touraille, G.D., McCarley, K.D., Bunge, A.L., Marty, J.-P., Guy, R.H., 2002. Percutaneous absorption of 4-cyanophenol from contaminated soil in vitro: effects of soil loading and contamination concentration. Regul. Toxicol. Pharmacol., submitted for publication.

Watkinson, A.C., Hadgraft, J., Walters, K.A., Brain, K.R., 1994. Measurement of diffusional parameters in membranes using ATR-FTIR spectroscopy. Int. J. Cosmetic Sci. 16, 199–210.